ACS Partner Journal

Journal of the American Society for Mass Spectrometry

pubs.acs.org/jasms

Research Article

Capillary Electrophoresis−High Resolution Mass Spectrometry for Measuring In Vivo Arginine Isotope Incorporation in Alzheimer's Disease Mouse Models

Kendra J. Adams, Joan G. Wilson, David S. Millington, M. Arthur Moseley, Carol A. Colton, J. Will Thompson,* and W. Kirby Gottschalk*

Cite This: https://doi.org/10.1021/jasms.1c00055

Read Online

ACCESS | Metrics & More | Article Recommendations | Supporting Information

ABSTRACT: Immune-based metabolic reprogramming of arginine utilization in the brain contributes to the neuronal pathology associated with Alzheimer's disease (AD). To enable our long-term goals of differentiation of AD mouse model genotypes, ages, and sexes based on activity of this pathway, we describe here the novel dosing (using uniformly labeled ($^{13}C_6{}^{15}N_4$) arginine) and analysis methods using capillary electrophoresis high-resolution accurate-mass mass spectrometry for isotope tracing of metabolic products of arginine. We developed a pseudoprimed infusion-dosing regimen, using repeated injections, to achieve a steady state of uniformly labeled arginine in 135−195 min post bolus dose. Incorporation of stable isotope labeled carbon and nitrogen from uniformly labeled arginine into a host of downstream metabolites was measured *in vivo* in mice using serially sampled dried blood spots from the tail. In addition to the dried blood spot time course samples, total isotope incorporation into arginine-related metabolites was measured in the whole brain and plasma after 285 min. Preliminary demonstration of the technique identified differences isotope incorporation in arginine metabolites between male and female mice in a mouse-model of sporadic Alzheimer's disease (APOE4/huNOS2). The technique described herein will permit arginine pathway activity differentiation between mouse genotypes, ages, sexes, or drug treatments in order to elucidate the contribution of this pathway to Alzheimer's disease.

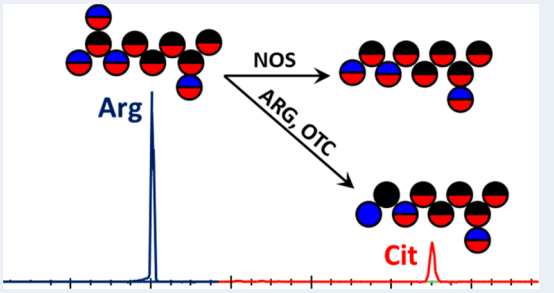

INTRODUCTION

The application of metabolic flux analysis to study normal biochemical pathways in cells and tissue permits exploration of targeted pathways and provides comparisons of metabolic differences between disease states. Flux analysis has been utilized for both *in vitro* and *in vivo* approaches in diverse applications ranging from nutritional studies,[1] cancer,[2] cerebral glutamate metabolism,[3] malaria, and sickle cell disease research in humans and mice,[4−6] observing functions of neural stem cells (NSCs) following transplantation[7] and metabolic tracing in mice.[8−10] Metabolic flux analysis is a powerful tool for tracing intermediary metabolites and uncovering how factors such as genotype, age, sex, disease, developmental stage, or pharmacological treatments govern metabolism. The application of metabolic flux analysis to Alzheimer's disease (AD) research is an important method for understanding the activity of pathways believed to be associated with the disease and potentially will allow interrogation of metabolic activity differences between normal individuals and those with AD. Accumulation of stable isotope labeled atoms from uniformly labeled arginine into other metabolites over time and along the pathways of interest will improve our knowledge of how pathways are modulated in association with disease, and provide a better understanding of AD disease mechanisms which involve arginine-related inflammation. We chose to design a study to specifically monitor arginine metabolism by dosing with uniformly labeled arginine and measuring stable isotope incorporation in the blood and the brains of the mice, with the goal of developing the dosing regimen and analytical tools required to investigate potential therapeutic targets of this pathway or other alterations which may affect the activity of this pathway such as biological sex or genetic differences.

Stable isotope tracing is performed by introducing a heavy isotope enriched compound to an *in vitro* or *in vivo* biological system and observing the incorporation of heavy atoms into downstream metabolites of interest. The technique can provide information on changes in metabolites that may occur when a metabolic pathway is altered. For example, Cerrada-Gimenez et al.[11] used heavy-labeled polyamine precursors (arginine, methionine, and ornithine) to measure changes in polyamine

Received: February 10, 2021
Revised: April 22, 2021
Accepted: May 11, 2021

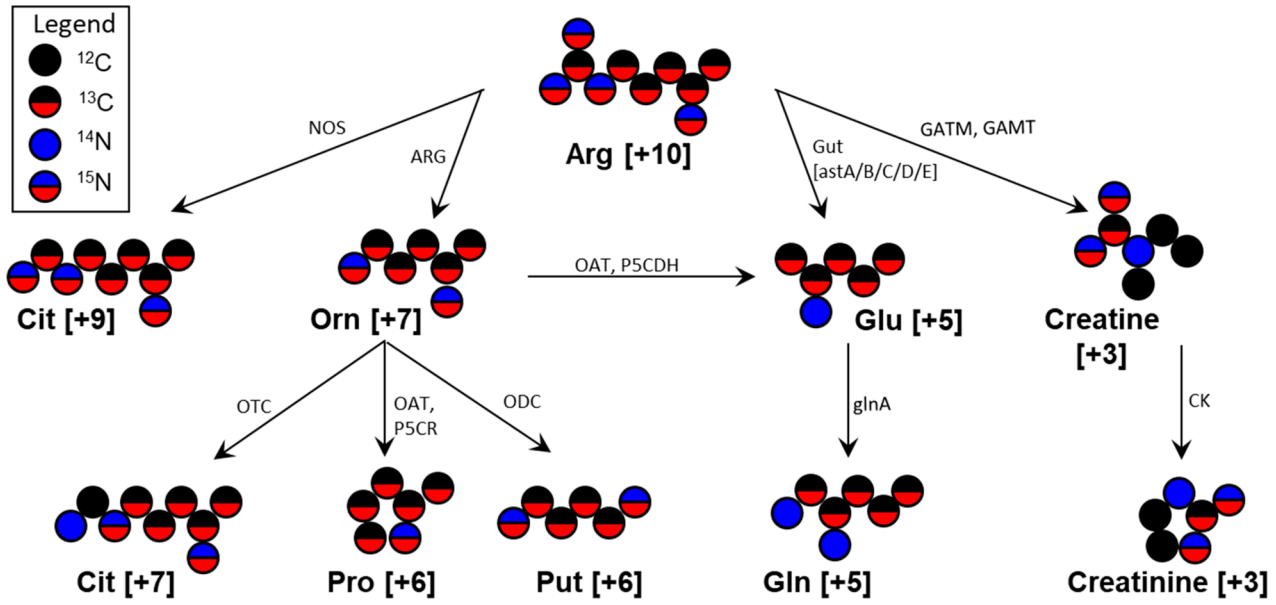

Figure 1. Carbon- and nitrogen-labeling pattern for key metabolites observed in the CE−MS isotope tracing experiments using universally ^{13}C- and ^{15}N-labeled arginine ("Arg [+10]"). Arginine +7 can also be observed from recycled citrulline. As noted in the legend, any stable-isotope containing atoms are half red. Oxygen and hydrogen are withheld for clarity, and nominal mass annotations are used for simplicity only; exact mass was utilized for data analysis. Detailed structures can be found in Supplementary Figure 1.

flux after altering the enzymatic activity of spermidine/spermine-N^1-acetyltransferase (SSAT). These experiments are typically performed using mass spectrometry coupled to liquid chromatography (LC) in order to increase sensitivity and specificity.[12−14] In some cases, limited amounts of available specimen and the challenges imposed by the nature of the target analytes (such as polarity) require more advanced techniques to effect accurate quantification of the target compounds. One helpful approach is capillary electrophoresis (CE), which separates compounds based on their electrophoretic mobility determined by the size and charge of the molecule, and generally provides good separation performance for polar compounds. Although CE−MS has previously been exclusively applied to metabolomics, major practical improvements have been introduced that make it an appealing alternative to LC−MS;[15−18] it has also been applied to stable isotope incorporation experiments.[19,20] In this study, the 908 Devices ZipChip capillary electrophoresis coupled to a ThermoScientific Q Exactive HF was used for arginine flux analysis, which has a high resolving power per unit time and uses a very simple sample preparation technique. The ZipChip CE−MS protocol has been utilized for proteomics approaches in cells, using low sample volume and rapid analysis.[21,22] The use of a HRAM mass spectrometer affords the opportunity to analyze the acquired data for many compounds in one or more pathways without additional sample consumption.[8,12−14,23]

We have developed multiple mouse models of Alzheimer's disease, including the AppSwDI/mNos2$^{-/-}$ (CVN) mouse strain which faithfully recapitulates the salient features of Alzheimer's disease pathology and the HuNOS2/mNos2$^{-/-}$ (HN) mouse strain which parallels human responses to inflammatory stimuli rather than typical mouse repsonses.[24−28] CVN mice are characterized by increased Arg1 gene expression at 12−24 weeks of age compared to control mice in combination with decreased arginine bioavailability (arginine/(ornithine+citrulline)).[29] The HN mouse includes the human NOS2 gene as a replacement for the mouse Nos2 gene and creates immune and oxidative stress responses in mice that better resemble human responses.[28] Changes in immunity and redox balance are both key features of neurodegenerative diseases including AD.[28,30] Arginine and its associated pathways have been targeted in human brain where levels of ornithine and urea[31] and polyamines and acetylated polyamines[32] are positively correlated with AD. Using untargeted LC−MS, Graham et al. discovered several polyamine and arginine pathway components in human plasma which distinguished the metabolic profiles of individuals diagnosed with mild cognitive impairment who converted to AD from nonconverters.[33] This and other work led us to hypothesize that a disrupted arginine pathway initiates and/or contributes to the neurodegenerative disease state. If true, then arginine or molecules in the associated metabolic pathways are potential biomarkers or drug targets for the disease process.[26,29,34,35] Identifying how these pathways change during the pathogenesis of AD and when those changes occur during the time course of the disease may lead to discoveries in specific causes of the disease aiding in earlier diagnoses and improved therapeutic interventions.

In this report, uniformly labeled $^{13}C_6{}^{15}N_4$-enriched arginine was utilized as a metabolic probe to determine the relative incorporation of ^{13}C and ^{15}N in the downstream metabolites of arginine. Figure 1 summarizes the major metabolic fates of arginine, as well as molecular locations of ^{13}C (red and black circle) and ^{15}N (red and blue circle) from uniformly labeled arginine. $^{13}C_6{}^{15}N_4$ arginine (arginine +10) forms $^{13}C_5{}^{15}N_2$ ornithine (ornithine +7) via arginase (ARG), subsequently converting to $^{13}C_5{}^{15}N_2$ citrulline (citrulline +7) via ornithine carbamoyltransferase (OTC). $^{13}C_6{}^{15}N_3$ citrulline (citrulline +9) is also derived from arginine +10 directly via nitric oxide synthase (NOS). With the fully labeled arginine +10 as a starting molecule, it is therefore possible to independently quantify citrulline produced via NOS (citrulline +9) and citrulline produced via ARG and OTC (citrulline +7) and critically verifies the ability of the method to differentiate

https://doi.org/10.1021/jasms.1c00055
J. Am. Soc. Mass Spectrom. XXXX, XXX, XXX−XXX

activity of these pathways based on genotype or phenotype.[29,36−42] In addition to citrulline, ornithine +7 converts to $^{13}C_5{}^{15}N$ proline (proline +6) through ornithine aminotransferase (OAT) and glutamate 5-semialdehyde dehydrogenase and contributes to the polyamine pathway via ornithine decarboxylase (ODC). Furthermore, $^{13}C^{15}N_2$ creatine (creatine +3) is formed directly from arginine +10 via glycine amidinotransferase (GATM) and guanidinoacetate *N*-methyltransferase (GAMT) and $^{13}C_5{}^{15}N$ creatinine (creatinine +3) from creatine +3 via creatine kinase (CK). Finally, arginine +10 is also metabolized to $^{13}C_5$ glutamate (glutamate +5) by two mechanisms, either in the gut (astA/B/C/D/E) or via ornithine (OAT and Δ^1-pyrroline-5-carboxylate dehydrogenase (P5CHD)). Glutamate +5 is then converted to $^{13}C_5$ glutamine (glutamine +5) via glutamine synthetase (gln *A*) (Figure 1). Ultimately, using this approach to measure incorporation levels in the whole blood, brain, and plasma in the HuNOS/mNOS$^{-/-}$ mouse and other AD mouse models may yield important insights into the relative activity of arginine metabolism and inflammation.

In this paper, we describe the sample preparation and CE−MS protocols developed for the metabolites of interest in plasma, dried blood spots, and whole brain tissue. Using bolus dosing, the half-life ($t_{1/2}$) of the $^{13}C_4{}^{15}N_6$ arginine was estimated in brain and blood. From this data, we optimized serial dosing levels and conditions for in vivo dosing of mice via repeated intraperitoneal (IP) injections as a surrogate for continuous infusion (which was deemed impractical in the animal model). The use of CE coupled to high-resolution accurate-mass mass spectrometry (HRAM-MS) allowed for rapid analysis of the samples with reliable results and the ability to reanalyze the data as other metabolites in the pathway become apparent and interesting. Finally, we performed proof-of-concept tracing measurements in a mouse model relevant to human AD research (APOE4 huNOS2 (E4HN), total n = 12 animals and 108 samples). We demonstrate that metabolic flux analysis using isotopically enriched arginine allows for tracing and analysis of compounds in vivo and may allow a deeper understanding of how and when these pathways and metabolites are altered in the disease state and between male and female mice.

EXPERIMENTAL SECTION

Materials. $^{13}C_6$, 99%; $^{15}N_4$, 99% L-arginine:HCl was purchased from Cambridge Isotope Laboratories (Andover, MA). All solvents used were of LC−MS grade or better; acetonitrile, water, chloroform, methanol and formic acid were purchased from Fisher Scientific (Pittsburgh, PA).

Animals and Dosing. All animal experiments were performed in accordance with protocols approved by the Institutional Animal Care and Use Committee (IACUC) at Duke University Medical Center under the National Institutes of Health Guide for the Utilization and Care of Vertebrate Animals Used in Testing, Research and Training. Mice used in the study were chosen to test the concept that genetic changes in key enzymes that determine metabolic pathways could impact metabolite distribution. In this case, we test a well-known enzyme system that permits evaluation of the initial use of arginine by two different but well-described pathways, that is, the competition for arginine by arginase (ARG1,2) and nitric oxide synthase 2 (NOS2).[43−45] To better apply this study to use in humans as well in mouse models of disease, we used mice that were genetically altered by replacing the mouse Nos2 (mNos2) gene with the human NOS2 gene (huNOS2). This genetic change allows this research to be more applicable to humans with disease and accounts for the large differences between arginine utilization by mNos2 compared to the corresponding human protein. Targeted replacement APOE4 mice faithfully recapitulate tissue-specific ApoE protein expression, unlike wild-type mice,[46] and exhibit synaptic and some cognitive deficits (summarized in ref 47) but do not exhibit widespread neuropathology.[48] All currently available APOE mouse models are wild type for Nos2, which is expressed at higher levels and is more active than the human orthologue (reviewed in ref 28). To mimic the human condition more faithfully in APOE4 mice, we replaced Nos2 with the human orthologue in targeted replacement APOE4 mice (hereinafter E4HN for: Human Nitric Oxide/APOE4 mice). To investigate arginine metabolic fate in mouse AD related models, we utilized NOS2/Nos2$^{-/-}$ (HN) mice, and APOE4 targeted replacement mice that possess the HN background (E4HN; Colton et al., manuscript in preparation). We used both male and female APOE4 huNOS2 (E4HN) mice at 69 weeks of age (n = 12, 6 male and 6 female).

Arginine Kinetics Experiment. Four 16-week old CVN mice were dosed with a bolus intraperitoneal (IP) injection of 5 mg/kg of $^{13}C_6$, 99%; $^{15}N_4$, 99% L-arginine:HCl (Cambridge Isotope Laboratories, Inc., Andover, MA) prepared in physiological saline. Plasma and brain samples were harvested from individual animals at T = 15, 45, 90, and 180 min after dosing. Mice were euthanized via exsanguination under lethal anesthesia (ketamine/xylazine). Blood was immediately collected for plasma analysis in sodium citrate tubes, and the brains were immediately perfused with saline, deposited directly into liquid nitrogen after removal from the skull, and stored at −80 °C. This experiment was not utilized for an absolute determination of $t_{1/2}$, and we therefore sacrificed one animal at each time point and performed two mass spectrometric measurements of each.

Steady-State Experiments. For the steady-state exploratory experiment, we used three male 40−52 week-old APOE3 targeted replacement mice, which have intact Nos2 but human APOE3 in place of the mouse ApoE.[49] Mice were treated with a bolus IP injection of 0.37 mg $^{13}C_6{}^{15}N_4$ arginine at T = 0 min (200 μL of a 1.87 mg/mL solution) followed by injections of 0.19 mg doses every 30 min from T = 15 min to T = 255 min (100 μL of 1.87 mg/mL). Thirty minutes following the last injection (T = 285 min) mice were euthanized as described above. Blood spots were collected from a tail snip at T = 0, 15, 45, 135, 195, 255, and 285 min, spotted directly onto Whatman 903 Proteinsaver cards, dried at room temperature overnight, and stored at 4 °C for DBS analysis; the plasma and brains were collected as described above.

Sample Preparation. Dried blood spots (∼3 mm) were punched out directly onto a 0.22 μm filter (Millipore) in a polypropylene collection tube. A 100 μL aliquot of metabolite sample diluent (908 Devices, Inc., Boston, MA) supplemented with 0.2 M ammonium acetate was added to the spots which were then incubated with shaking using a Thermomixer (750 rpm) at room temperature for 30 min. The filter tubes were then centrifuged for 5 min at ∼15000 rcf, and approximately 80 μL of filtrate was collected and transferred to glass total recovery auto sampler vials (Waters Corp., Milford, MA).

Twenty microliters of plasma was diluted with 140 μL of methanol plus 40 μL of 0.5 M ammonium acetate. Samples were shaken at 37 °C for 10 min (750 rpm), cooled to 4 °C

https://doi.org/10.1021/jasms.1c00055
J. Am. Soc. Mass Spectrom. XXXX, XXX, XXX−XXX

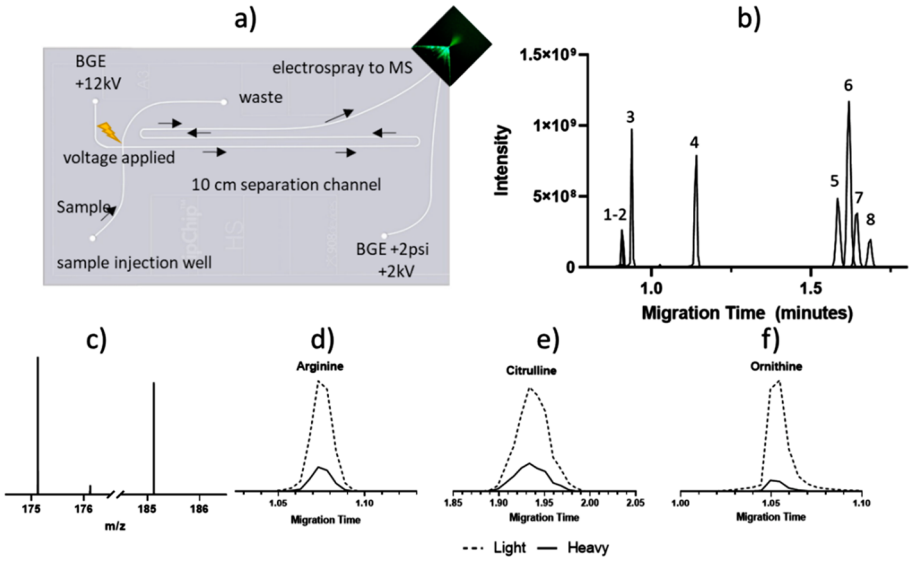

Figure 2. (a) ZipChip device used for capillary electrophoresis and sample introduction (note real time electrospray view in top right corner). Chip is made out of glass with an etched channel for sample transportation and separation. Voltage is applied to the chip, which directs positively charged compounds toward the mass spectrometer and negatively charged and neutral compounds into the designated waste wells. (b) Electropherogram of (1) ornithine, (2) creatinine, (3) arginine, (4) creatine, (5) proline, (6) glutamine, (7) glutamate, and (8) citrulline throughout a 2 min electrophoretic separation time. (c) MS1 spectrum for endogenous ("light") arginine (m/z 175) and uniformly stable labeled ("heavy") arginine (m/z 185). (d–f) Electrophoretic peaks for "light" and "heavy" arginine, citrulline, and ornithine. Image in (a) provided by 908 Devices, Inc.

over dry ice, and spun at 20000 rcf for 10 min at 4 °C. One hundred microliters of clear supernatant was transferred to glass total recovery autosampler vials (Waters Corp).

Brain samples were weighed into a Precellys CK14 Lysing Kit for soft tissue homogenizing (Bertin Corp. Montigny-le-Bretonneux, France), and 100 μL of 50/50 MeOH/H_2O per 50 mg of brain tissue was added to each sample. Sample weights were between 0.394 and 0.518 g. The samples were homogenized in a Precellys Evolution Homogenizer (Bertin Corp. Montigny-le-Bretonneux, France) for three cycles of 10 s at 10000 rpm at 4 °C with 60 s cooling time between cycles. Samples were removed from the homogenizer, and a 100 μL aliquot of the primary homogenate was combined with 250 μL of 3:1 MeOH/$CHCl_3$ in a new CK14 tube, and homogenization was repeated. Samples of the final homogenate were centrifuged at 10000 rcf and 4 °C for 10 min. Approximately 100 μL of supernatant was removed and combined with 10 μL of 2 M ammonium acetate in glass total recovery autosampler vials (Waters Corp.).

CE–MS Analysis. Analysis was performed by capillary electrophoresis mass spectrometry (CE–MS) utilizing a ZipChip CE system (908 Devices, Inc. Boston, MA) and a Q Exactive HF mass spectrometer (ThermoFisher Waltham, MA). Metabolite background electrolyte (Metabolite BGE, 908 Devices, Inc.) and an HS Chip were used for the CE separation (908 Devices, Inc.). The separation was performed with 1000 V/cm and 8 nL injection volume. Total separation time was 4 min, with pressure assist activated at 2 min. Electrospray ionization in positive mode was used for introduction into the Q Exactive HF, and two mass spectrometric analyses were performed per sample injection using MS1 scans at different resolutions (Rs), 120k and 240k, with 3e6 AGC target. A SIM scan from m/z 180–190 was used for the collection of the 240k results, whereas a mass range of 70–500 m/z was utilized for the 120k collection. For the results shown below, the 120k data was used to calculate incorporation for arginine, ornithine, creatine, creatinine, proline, glutamate, and glutamine, while the 240k method was utilized for citrulline in order to remove interferences that cause quantification difficulties for citrulline +9 at lower resolution. We uploaded the raw data to www.panoramaweb.org under the project "CE–MS for Measuring in vivo Arginine Isotope Incorporation in Alzheimer's Disease Mouse Models" (https://panoramaweb.org/tczcoD.url).

The ZipChip includes an autosampler and a glass microfluidic CE chip. This chip is coupled directly with the inlet of the Orbitrap via electrospray ionization, resulting in a zero-loss interface between the separation and detection. The ZipChip contains several wells that are etched into the glass chip, one for sample injection, others for waste of neutral and negatively charged molecules, and BGE. A 10 cm long channel is used for electrophoretic separation of the metabolites. The ZipChip was built to perform microfluidics through capillary channels in which compounds migrate and are separated based on their size and charge and are introduced into the mass spectrometer via electrospray ionization at the corner of the chip, which can viewed in real time using the 908 Devices ZipChip software (Figure 2a).[18,50]

Data Processing. *Calculating Incorporation.* Data analysis in the form of peak area extraction of metabolites of interest was performed from the *.raw mass spectrometry files using Skyline Daily versions 4.1.1.18257, 4.2.1.19058, and 19.1.9.350.[51] Skyline was provided with the molecular formula, ionization adduct ($[M + H]^+$), and expected migration time of each molecule of interest, along with instructions to extract data 120000 resolving power (m/z 200). Following peak integration in Skyline, incorporation ratios are reported as the peak area of the heavy isotope divided by the total peak area, where the total peak area is the sum of the peak area of naturally occurring isotopes with relative abundance greater than 0.1%, as well as the heavy isotope peak.

$$\%\ \text{incorporation} = \frac{\text{peak area of heavy isotope}}{\text{total peak area}} \times 100 \quad (1)$$

https://doi.org/10.1021/jasms.1c00055
J. Am. Soc. Mass Spectrom. XXXX, XXX, XXX–XXX

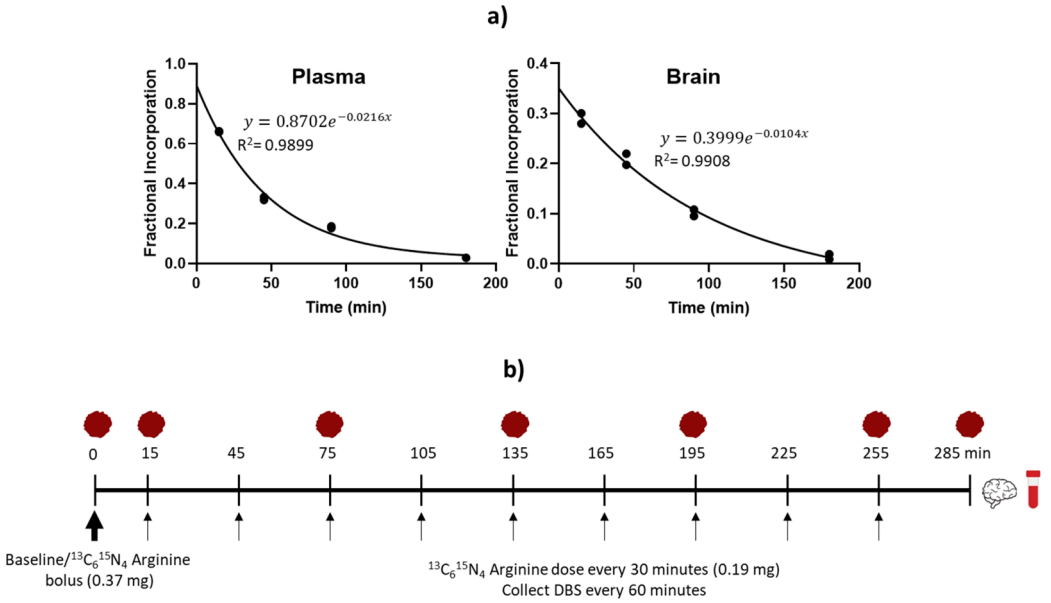

Figure 3. (a) Fractional isotope incorporation of $^{13}C_6{}^{15}N_4$ arginine after single bolus dose in CVN mice performed to approximate arginine half-life (n = 1 per time point). Half-life ($t_{1/2}$) is measured as 32.1 and 66.7 min in plasma and brain, respectively. (b) Experimental design timeline for semicontinuous dosing of $^{13}C_6{}^{15}N_4$ arginine, along with sample collection regimen; arrows represent dosing with $^{13}C_6{}^{15}N_4$ arginine; red spots represent collection of dried blood spots; brain and vial icons represent collection of brain and plasma. Two measurements were performed at each time point.

The total intensity for the native monoisotopic form (A) was corrected to include the expected native contribution of ^{13}C and ^{15}N to arginine (A+1, 8.25%; A+2, 0.71%), citrulline (A+1, 7.91%; A+2, 0.89%), ornithine (A+1, 6.4%; A+2, 0.59%), creatine (A+1, 6.0%; A+2, 0.56%), creatinine (A+1, 5.6%; A+2, 0.34%), proline (A+1, 5.7%; A+2, 0.54%), glutamate (A+1, 5.6%; A+2, 0.91%), and glutamine (A+1, 5.7%; A+2, 0.73%). Skyline files for the pilot kinetics experiment, pilot APOE3 experiment, and the E4HN mouse experiment have been uploaded to Panorama (https://panoramaweb.org/tczcoD.url).

Cumulative Incorporation Calculations. Differences in isotope incorporation of the arginine derivatives during continuous infusion make it difficult to fit a curve to the DBS data. Some compounds may show high amounts of enriched isotope incorporation within 15 min of the bolus dose, whereas others that are further downstream from arginine in the metabolic pathway may not have measurable incorporations until a later time point. Therefore, we chose to measure the total incorporation over time for each metabolite by calculating the area under % incorporation curve (AUC) in the DBS over the entire data collection window of 285 min using GraphPad Prism 8.3.0. To correct for potential differences in downstream metabolites which resulted from variance in the available isotope-labeled arginine pool (from slight dosing differences), the percent incorporation of each compound was normalized to the % incorporation of arginine +10 and then we calculated the AUC (see Supplementary Table 1). We found that using the cumulative incorporation of the heavy isotopes over time decreased between-animal variance, enabling more accurate comparisons between individual animals, genotypes, sexes, and ages for each metabolite.

RESULTS AND DISCUSSION

CE−MS for Isotope Incorporation. Capillary electrophoresis coupled to high-resolution mass spectrometry (CE-HR MS) was used for the analysis and detection of the heavy labeled downstream metabolites of arginine. The migration times of each of the metabolites ranged from 0.85 to 1.85 min with baseline separation between most of the analytes of interest. The elution order of the eight compounds we focused on in this analysis was ornithine, creatinine, arginine, creatine, proline, glutamine, glutamate, and citrulline, and width at half height was on average 0.012 min, demonstrating a chromatographic peak capacity of 83 during the ∼60 s elution period of these metabolites (Figure 2B). The partial mass spectrum of endogenous arginine at the time of arginine elution (0.9 min) is shown in Figure 2c. Protonated arginine (m/z 175.1190) coeluted with uniformly labeled arginine (m/z 185.1272) during CE separation. Electrophoretic peaks corresponding to the endogenous (light) protonated molecular ions of arginine, citrulline and ornithine (dotted lines) with their corresponding coeluting heavy isotopes (solid lines) are shown in Figure 2d−f and demonstrate between 5 (arginine) and 9 (citrulline) MS data points across the chromatographic peak at 120,000 Rs setting on the Q Exactive HF.

Detecting Isotope Incorporations into Mouse: Designing Dosing Regimen. Initial experiments were designed to maximize the capability to independently determine biochemical isotope incorporation in the plasma and the brain and to estimate the half-lives ($t_{1/2}$) of the relevant compounds in plasma and brain tissue by optimizing the dosing regimen, the extraction procedure, and CE/MS conditions. The tissue-specific turnover of arginine was approximated using a pharmacokinetic-type experiment to determine the dosing schedule required to achieve a pseudo-steady state of isotope enriched arginine incorporation. After a bolus dose of $^{13}C_6{}^{15}N_4$ arginine, the animals were euthanized at 15, 45, 90, and 180 min post dose, and plasma and brains

https://doi.org/10.1021/jasms.1c00055
J. Am. Soc. Mass Spectrom. XXXX, XXX, XXX−XXX

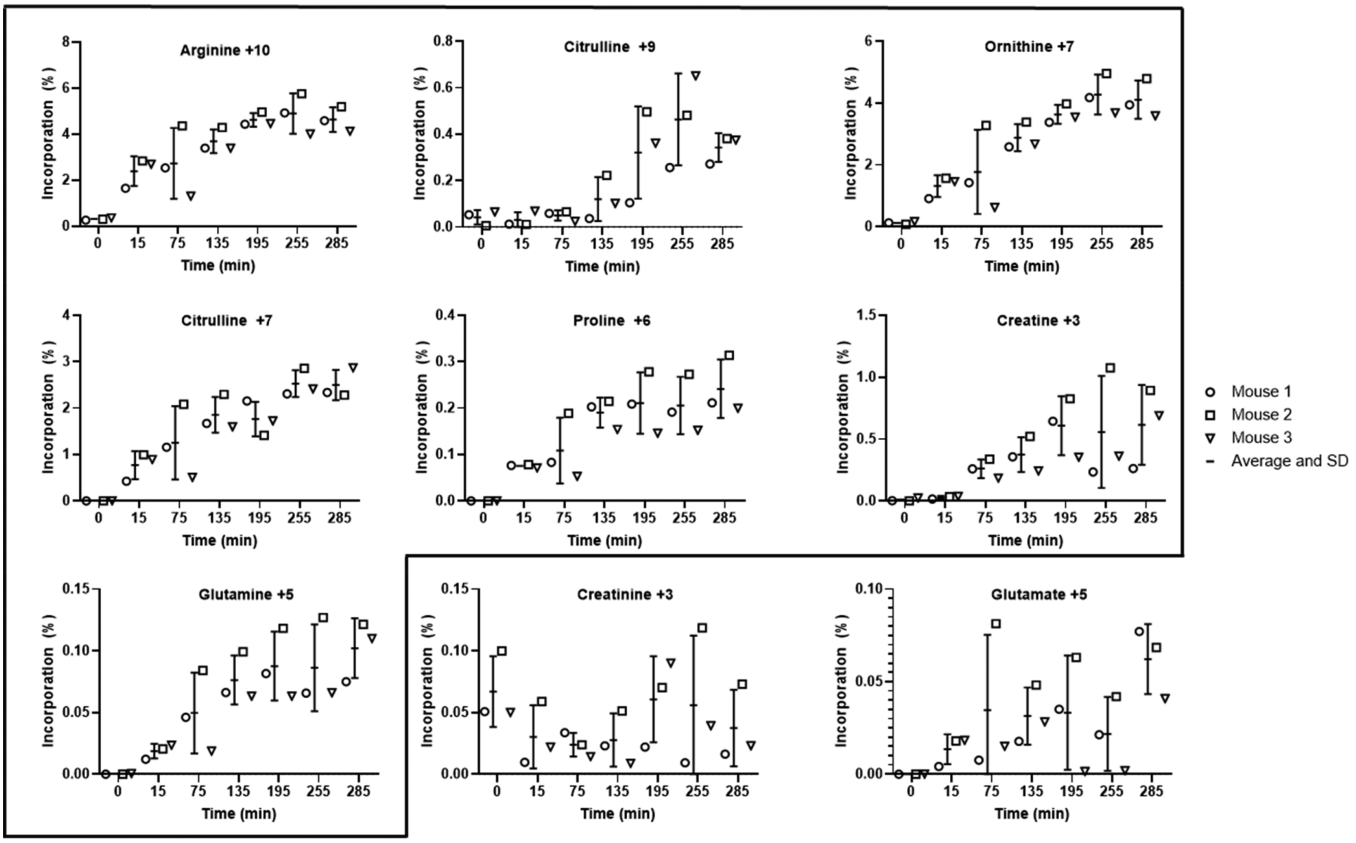

Figure 4. Stable isotope enrichments in dried blood spots as a function of time. Male APOE3 mice ($N = 3$) were dosed IP with $^{13}C_6{}^{15}N_4$ arginine (0.37 mg bolus dose and serial injections of 0.19 mg at the times indicated in Figure 3b). Percent incorporation shown for arginine, citrulline +9, ornithine, citrulline +7, proline +6, creatine +3, creatinine +3, glutamine +5 and glutamate +5. Incorporation amounts and time to reach a steady state of incorporation (if at all) vary for each metabolite. Creatinine and glutamate did not show a reliable incorporation into the blood.

were collected. The fractional incorporations of $^{13}C_6{}^{15}N_4$ arginine were calculated using the formula in eq 1. We obtained the approximate $t_{1/2}$ in each of the matrices by fitting the fractional incorporations to a first-order exponential decay curve (Figure 3a). The $t_{1/2}$ of arginine+10 was calculated as 32.1 min in the plasma and 66.7 min in the brain. These results are in agreement with published reports from other species, in which the half-life of arginine in plasma and serum after intravenous infusions ranged from 45 min to 1 h in ewes, rats, pigs, and humans.[52,53] Using these results, an arginine dosing schedule was developed to achieve a steady-state enrichment of heavy isotope labeled arginine in the treated mice as shown in Figure 3b. A bolus dose was administered followed by several smaller doses at 30 min intervals. On the basis of the calculated $t_{1/2}$ for plasma, dosing at these intervals should allow the isotope-enriched arginine to reach a pseudo-steady state of incorporation.

Detecting Isotope Incorporations into Mouse: Longitudinal Dosing Experiments Reaching Steady State. Incorporation of $^{13}C_6{}^{15}N_4$ arginine in the arginine pool in DBS was monitored over the 4.5 h dosing regimen established in Figure 3b in a group of three APOE3 mice. Importantly, these animals express the mouse form(s) of nitric oxide synthase, Nos, which many of our other AD model animals do not. This was necessary in order to demonstrate that if citrulline+9 were being produced via nitric oxide synthase, we would be able to detect it. We calculated the percent incorporation relative to the native metabolite (eq 1) for arginine +10 and arginine pathway metabolites (see Figure 1) at seven time points. We were able to measure heavy isotope incorporation in arginine pathway metabolites including ornithine +7, citrulline +7, citrulline +9, proline +6, creatine +3, creatinine +3, glutamine +5, and glutamate +5. Overall, % incorporation for several of the compounds reached a plateau (steady state) in blood at or before $T = 285$ min (Figure 4).

Incorporation ratios for all compounds are negligible for the samples taken before administration at $T = 0$ min, providing a baseline incorporation level (limit of detection); the average incorporation LOD across the compounds in Figure 4 was 0.18%. In general, the blood collected 15 min postbolus dose already shows easily measurable levels of incorporation of the heavy isotopes in a majority of the compounds, excluding citrulline +9, creatine +3, creatinine +3 and glutamate +5. Formation of citrulline +9 is a measure of the NOS pathway and is a secondary route to citrulline formation, bypassing formation from ornithine; by contrast, citrulline+7 is a surrogate measure for the ARG/OTC pathway. Creatine, creatinine, and glutamate are further downstream from arginine than many of the other compounds, and this may contribute to low incorporations in those compounds at the early collection points. Creatinine +3 and glutamate +5 should be observable using arginine+10 dosing, they were not reliably detected in APOE3 mice over the dosing period in this pilot experiment, with incorporation levels <0.1% (see Figure 4).

Blood levels of arginine reached a steady state (plateau) of 5.1% incorporation between 195 and 255 min following the bolus dose. The isotope incorporation was 2.4% immediately following the bolus injection and approached the steady state

https://doi.org/10.1021/jasms.1c00055
J. Am. Soc. Mass Spectrom. XXXX, XXX, XXX−XXX

Table 1. Incorporation Percent of Stable Isotope for Arginine and Downstream Metabolites for Serially Sampled Dried Blood Spots, Brain, and Plasma from Male APOE3 Mice (N = 3)

	dried blood spots							brain	plasma
	T0	T15	T75	T135	T195	T255	T285	T285	T285
arginine+10	0.31 ± 0.05	2.4 ± 0.65	2.73 ± 1.54	3.69 ± 0.52	4.62 ± 0.29	4.9 ± 0.87	4.64 ± 0.54	2.34 ± 0.08	5.26 ± 0.66
citrulline+7	0.00 ± 0.00	0.77 ± 0.3	1.25 ± 0.79	1.85 ± 0.38	1.76 ± 0.37	2.53 ± 0.29	2.50 ± 0.33	1.23 ± 0.45	2.74 ± 0.68
citrulline+9	0.04 ± 0.03	0.03 ± 0.03	0.05 ± 0.02	0.12 ± 0.09	0.32 ± 0.2	0.46 ± 0.02	0.34 ± 0.06	1.52 ± 0.09	0.60 ± 0.24
ornithine+7	0.12 ± 0.04	1.32 ± 0.35	1.77 ± 1.36	2.88 ± 0.44	3.64 ± 0.31	4.28 ± 0.64	4.11 ± 0.62	5.92 ± 7.51	5.23 ± 0.5
creatine+3	0.01 ± 0.01	0.03 ± 0.01	0.26 ± 0.08	0.37 ± 0.14	0.61 ± 0.24	0.56 ± 0.45	0.61 ± 0.32	0.02 ± 0	0.81 ± 0.54
proline+6	0 ± 0	0.08 ± 0	0.12 ± 0.07	0.19 ± 0.03	0.21 ± 0.07	0.21 ± 0.06	0.24 ± 0.06	0.06 ± 0.03	0.22 ± 0.05
creatinine+3	0.07 ± 0.03	0.03 ± 0.03	0.02 ± 0.01	0.03 ± 0.02	0.06 ± 0.03	0.06 ± 0.06	0.04 ± 0.03	0.02 ± 0.01	0.20 ± 0.32
glutamine+5	0.00 ± 0.00	0.02 ± 0.01	0.05 ± 0.03	0.08 ± 0.02	0.09 ± 0.05	0.09 ± 0.05	0.10 ± 0.05	0.01 ± 0.00	0.12 ± 0.03
glutamate+5	0.00 ± 0.00	0.01 ± 0.01	0.03 ± 0.04	0.03 ± 0.02	0.03 ± 0.03	0.02 ± 0.02	0.06 ± 0.03	0.00 ± 0.00	0.01 ± 0.00

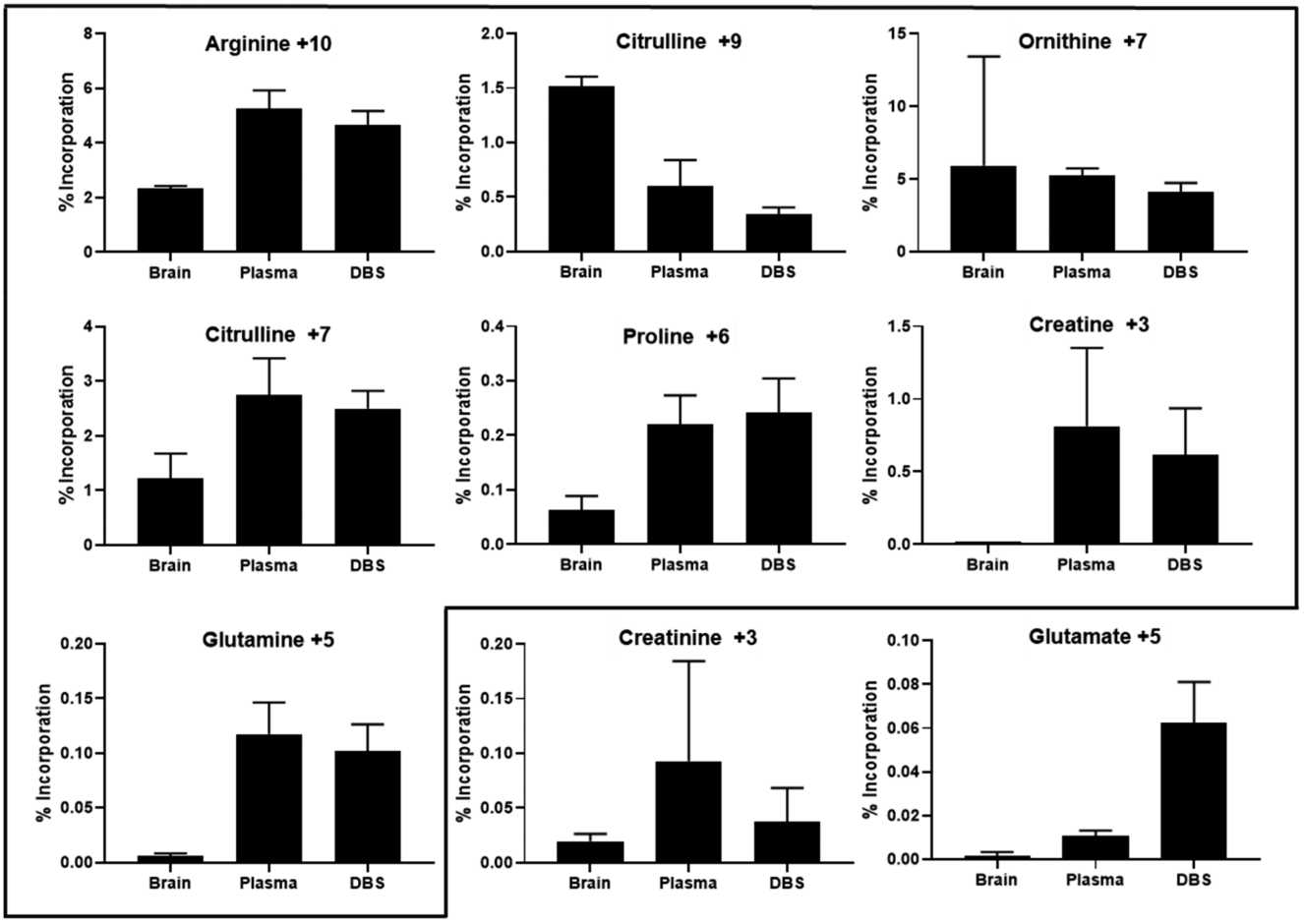

Figure 5. Terminal stable isotope enrichment in brain, plasma, and dried blood spot for arginine, citrulline +9, ornithine, citrulline +7, proline, creatine, creatinine, glutamine, and glutamate from male APOE3 mice (N = 3).

over the next 3 h of dosing (Figure 4). Ornithine +7 and citrulline +7 reached steady-state incorporation of 5.6% and 2.9% at 255 and 285 min, respectively, and the pattern of incorporation (shapes of the incorporation curves) of the heavy labels is similar to that of arginine (Figure 4). The isotope incorporation into citrulline +9 via NOS was delayed until ca. 135 min (Figure 4 and Table 1), after which it increased rapidly and reached incorporation of ~0.4% between 255 and 285 min. Previous studies of NO production using isotopic labeling claim about 1% of total arginine is converted to citrulline and NO (citrulline +9 in our study) and reached a steady state between 5 and 6 h with a primed continuous infusion of enriched arginine.[40,41] The biological relevance of the delay is under investigation. Incorporation into creatine +3 and proline +6 reach steady states of about 0.8% and 0.2%, respectively, between 255 and 285 min.

Due to animal husbandry requirements, serial sampling from whole blood was the only option for obtaining time course data for the current experiment. Dried blood spot (DBS) analysis affords the ability to use the same mouse for serial sampling, permitting the measurement of circulating arginine while minimizing the required number of animals. This also likely reduces the effects of animal-to-animal variation. In addition, using intermediate dosing and DBS obviates the need

https://doi.org/10.1021/jasms.1c00055
J. Am. Soc. Mass Spectrom. XXXX, XXX, XXX−XXX

to anesthetize the animals, which may affect the biological pathways. The disadvantage of this approach is that we are not able to measure time course incorporation in the brain.

To detect tissue-specific differences in the final steady-state incorporations, we harvested plasma and brains from each mouse at the conclusion of the experiment (T = 285 min). Comparison of the final fractional incorporations in each of the matrices (DBS, plasma and brain) is shown in Figure 5 (average ± standard deviation) and summarized in Table 1. For each compound, the plasma and DBS final incorporation values are comparable within both "types" of blood specimen. For the majority of the compounds analyzed, plasma and DBS incorporation ratios are equivalent after the 285 min, with the plasma and DBS values falling within the standard deviations of each other for the compounds reported. This supports the hypothesis that serial DBS collection is a useful method to perform longitudinal sampling of metabolites and isotope incorporation in circulation, requiring fewer animals and lower cost than sacrificing an animal at each time point. Moreover, for most compounds the final steady-state measurement in plasma is significantly different from brain tissue, validating that we can distinguish brain-specific metabolic effects from whole body effects, which are reflected in the blood/plasma samples. The final incorporation levels in the brain are generally lower than that of plasma or DBS, which is expected from the initial PK data showing brain turnover of arginine is slower than measured in circulation (Figure 3a). Additionally, the blood-brain-barrier and brain specific transporters likely play roles in the brain turnover of arginine.

Detecting Isotope Incorporations in Mice: Comparison of Incorporations in Alzheimer's Disease Mouse Models. We used the protocol validated in the previous sections to begin analyzing the interrelationships between arginine metabolism and Alzheimer's pathobiology. The APOE4 gene is the most significant known genetic risk factor for humans developing AD. For these experiments, we compared arginine metabolism in 69-week old E4HN mice between male and female (n = 6 each) animals to observe potential sex differences in pathway activity within this genotype. We compared the total incorporation of each metabolite over the time course, correcting for slight variability in the arginine+10 pool available within each animal, which was presumably due to small differences in dosing or uptake of the isotope from the IP injection.

Sex Differences. When corrected to the initial arginine+10 pool available incorporation in dried blood spots, we observed statistically significant differences in several arginine pathway metabolites (Table 2). Significantly higher incorporation of the isotope enrichment toward citrulline +7, and arginine +7 (recycled from citrulline+7 via argino-succinate) as well as glutamate and glutamine in females compared to males of the same age and genotype. Previous studies have reported an increase in arginase activity caused by testosterone, and NO synthesis in urine tends to be higher in females compared to males although no differences in total levels of arterial arginine, citrulline, or ornithine were observed.[10,54,55] While only half of the measured metabolites pass statistical significance between male and female animals (p-value <0.01), it is important to note that metabolites further downstream from the dosed isotope show more significant increase in females and more demonstrative statistical confidence. This is highly suggestive of increased overall metabolic activity of the ARG/OTC/OAT axis in female E4HN animals versus males. As we expected, incorporation of citrulline +9 was not observed for these genotypes of mice, because mouse NOS is replaced with the human gene which has lower activity human and shifts the metabolism away from citrulline +9.[28]

Table 2. Average Calculated Area under the Curve for 69 Week Old Female E4HN (6) and Male E4HN (n = 6) Mice, the Fold Change between them and the p-Value of the Differences between the Isotope-Enriched Metabolites Normalized to Enriched Arginine Incorporation

	female E4HN 69 wks vs male E4HN 69 wks total incorporations over time			
	avg M69E4HN	avg F69E4HN	fold change	p-value
Orn/Arg	200.32 ± 14.16	207.43 ± 13.20	1.04	0.389
Cit+7/Arg	108.85 ± 5.90	127.53 ± 11.31	1.17	0.005
Pro/Arg	12.36 ± 1.76	15.15 ± 2.72	1.22	0.062
creatine/Arg	29.85 ± 4.79	38.15 ± 4.63	1.28	0.012
creatinine/Arg	19.84 ± 5.19	24.51 ± 4.46	1.24	0.126
Glu/Arg	2.98 ± 0.33	4.38 ± 0.49	1.47	0.0002
GlnArg	6.99 ± 0.50	9.77 ± 1.11	1.40	0.0002
Arg+7/Arg	25.79 ± 3.05	34.92 ± 2.56	1.35	0.0002

CONCLUSIONS

This report provides a framework for investigating in vivo stable isotope labeling in mice, specifically for tracing the downstream metabolites of arginine in the blood, plasma, and brain tissue of mouse models of Alzheimer's disease. Based on the calculated half-life of the isotope enriched $^{13}C_6{}^{15}N_4$ arginine, a dosing scheme was developed to mimic primed infusion, and serial sampling via DBS allowed for monitoring of isotope incorporation into the metabolites over time. With the utilization of DBS for time course analysis, less animals and time are used for studies and biological effects are likely reduced when comparing the same exact animal over time. Although we were able to perform isotope tracing into the majority of canonical metabolic products of arginine, we are also interested in compounds even further downstream from arginine including polyamines like putrescine, spermidine, and spermine as well as their acetylated forms. With the current dosing regimen, we were unable to detect isotope enrichment of these compounds, and in future works a different dosing compound such as methionine or ornithine may be utilized or a longer time course may be needed in order to trace further downstream. Differences in the incorporations over time are reported between Alzheimer's disease related mouse models and sexes of mice. Significant differences are observed between 69-week-old E4HN female and male mice, with female mice incorporating significantly more citrulline +7 and arginine +7 over the dosing time course compared to the male mice. Using this technique, changes in metabolism between different genotypes, sexes, and ages can be revealed. This research provides method development techniques and tools for future stable isotope incorporation experiments for Alzheimer's disease research.

ASSOCIATED CONTENT

Supporting Information

The Supporting Information is available free of charge at https://pubs.acs.org/doi/10.1021/jasms.1c00055.

https://doi.org/10.1021/jasms.1c00055
J. Am. Soc. Mass Spectrom. XXXX, XXX, XXX−XXX

Detailed structures for key metabolites observed in the CE−MS tracing experiments using uniformly labeled $^{13}C_6{}^{15}N_4$ arginine (Figure S1), percent incorporation of enriched isotopes normalized to arginine +10 incorporation (Table S1) (PDF)

AUTHOR INFORMATION

Corresponding Authors

J. Will Thompson − *Proteomics and Metabolomics Shared Resource and Department of Pharmacology and Cancer Biology, Duke University, Durham, North Carolina 27710, United States;* orcid.org/0000-0001-6567-1268; Email: will.thompson@duke.edu

W. Kirby Gottschalk − *Department of Neurology, Duke University, Durham, North Carolina 27710, United States;* Email: kirby.gottschalk@duke.edu

Authors

Kendra J. Adams − *Proteomics and Metabolomics Shared Resource, Duke University, Durham, North Carolina 27710, United States*

Joan G. Wilson − *Department of Neurology, Duke University, Durham, North Carolina 27710, United States*

David S. Millington − *Department of Pediatrics, Duke University School of Medicine, Durham, North Carolina 27710, United States*

M. Arthur Moseley − *Proteomics and Metabolomics Shared Resource, Duke University, Durham, North Carolina 27710, United States*

Carol A. Colton − *Department of Neurology, Duke University, Durham, North Carolina 27710, United States*

Complete contact information is available at: https://pubs.acs.org/10.1021/jasms.1c00055

Notes

The authors declare no competing financial interest.

A Panorama Public project is associated with this manuscript: "CE−MS for Measuring in vivo Arginine Isotope Incorporation in Alzheimer's Disease Mouse Models" (https://panoramaweb.org/tczcoD.url).

ACKNOWLEDGMENTS

We gratefully acknowledge the Duke Proteomics and Metabolomics Core Facility and Thermofisher Scientific for access to the Q Exactive HF used in this work. We thank J. Scott Mellors at 908 Devices, Inc. for helpful conversations and guidance on best utilization of the ZipChip CE system. This work was supported by NIH R01 (RF1-AG057895-01A1) to C.A.C., W.K.G., and J.W.T.

REFERENCES

(1) Schoenheimer, R.; Rittenberg, D. Deuterium as an indicator in the study of intermediary metabolism. 6. Synthesis and destruction of fatty acids in the organism. *J. Biol. Chem.* **1936**, *114*, 381−396.

(2) Bruntz, R. C.; Lane, A. N.; Higashi, R. M.; Fan, T. W.-M. Exploring cancer metabolism using stable isotope-resolved metabolomics (SIRM). *J. Biol. Chem.* **2017**, *292* (28), 11601−11609.

(3) Sibson, N.; Dhankhar, A.; Mason, G.; Behar, K.; Rothman, D.; Shulman, R. In vivo 13C NMR measurements of cerebral glutamine synthesis as evidence for glutamate-glutamine cycling. *Proc. Natl. Acad. Sci. U. S. A.* **1997**, *94*, 2699−2704.

(4) Rubach, M. P.; Zhang, H.; Florence, S. M.; Mukemba, J. P.; Kalingonji, A. R.; Anstey, N. M.; Yeo, T. W.; Lopansri, B. K.; Thompson, J. W.; Mwaikambo, E. D.; Young, S.; Millington, D. S.; Weinberg, J. B.; Granger, D. L. Kinetic and Cross-Sectional Studies on the Genesis of Hypoargininemia in Severe Pediatric Plasmodium falciparum Malaria. *Infect. Immun.* **2019**, *87* (4), e00655−18.

(5) Marealle, A. I.; Siervo, M.; Wassel, S.; Bluck, L.; Prentice, A. M.; Minzi, O.; Sasi, P.; Kamuhabwa, A.; Soka, D.; Makani, J.; Cox, S. E. A pilot study of a non-invasive oral nitrate stable isotopic method suggests that arginine and citrulline supplementation increases whole-body NO production in Tanzanian children with sickle cell disease. *Nitric Oxide* **2018**, *74*, 19−22.

(6) Alkaitis, M. S.; Wang, H.; Ikeda, A. K.; Rowley, C. A.; MacCormick, I. J.; Chertow, J. H.; Billker, O.; Suffredini, A. F.; Roberts, D. J.; Taylor, T. E.; Seydel, K. B.; Ackerman, H. C. Decreased rate of plasma arginine appearance in murine malaria may explain hypoargininemia in children with cerebral malaria. *J. Infect. Dis.* **2016**, *214* (12), 1840−1849.

(7) Drago, D.; Basso, V.; Gaude, E.; Volpe, G.; Peruzzotti-Jametti, L.; Bachi, A.; Musco, G.; Andolfo, A.; Frezza, C.; Mondino, A.; Pluchino, S. Metabolic determinants of the immune modulatory function of neural stem cells. *J. Neuroinflammation* **2016**, *13* (1), 232.

(8) Sun, R. C.; Fan, T. W.-M.; Deng, P.; Higashi, R. M.; Lane, A. N.; Le, A.-T.; Scott, T. L.; Sun, Q.; Warmoes, M. O.; Yang, Y. Noninvasive liquid diet delivery of stable isotopes into mouse models for deep metabolic network tracing. *Nat. Commun.* **2017**, *8* (1), 1646.

(9) Grasemann, H.; Jaecklin, T.; Mehl, A.; Huang, H.; Rafii, M.; Pencharz, P.; Ratjen, F. Multitracer stable isotope quantification of arginase and nitric oxide synthase activity in a mouse model of pseudomonas lung infection. *Mediators Inflammation* **2014**, *2014*, 1.

(10) Luiking, Y.; Hallemeesch, M.; Vissers, Y.; Lamers, W.; Deutz, N. In vivo whole body and organ arginine metabolism during endotoxemia (sepsis) is dependent on mouse strain and gender. *J. Nutr.* **2004**, *134* (10), 2768S−2774S.

(11) Cerrada-Gimenez, M.; Häkkinen, M. R.; Vepsäläinen, J.; Auriola, S.; Alhonen, L.; Keinänen, T. A. Polyamine flux analysis by determination of heavy isotope incorporation from 13 C, 15 N-enriched amino acids into polyamines by LC−MS/MS. *Amino Acids* **2012**, *42* (2−3), 451−460.

(12) Jang, C.; Chen, L.; Rabinowitz, J. D. Metabolomics and isotope tracing. *Cell* **2018**, *173* (4), 822−837.

(13) Reisz, J. A.; D'Alessandro, A. Measurement of metabolic fluxes using stable isotope tracers in whole animals and human patients. *Curr. Opin. Clin. Nutr. Metab. Care* **2017**, *20* (5), 366−374.

(14) Balcells, C.; Foguet, C.; Tarragó-Celada, J.; de Atauri, P.; Marin, S.; Cascante, M. Tracing metabolic fluxes using mass spectrometry: stable isotope-resolved metabolomics in health and disease. *TrAC, Trends Anal. Chem.* **2019**, *120*, 115371.

(15) Zhang, W.; Hankemeier, T.; Ramautar, R. Next-generation capillary electrophoresis−mass spectrometry approaches in metabolomics. *Curr. Opin. Biotechnol.* **2017**, *43*, 1−7.

(16) Mellors, J.; Gorbounov, V.; Ramsey, R.; Ramsey, J. Fully integrated glass microfluidic device for performing high-efficiency capillary electrophoresis and electrospray ionization mass spectrometry. *Anal. Chem.* **2008**, *80* (18), 6881−6887.

(17) Soga, T.; Ohashi, Y.; Ueno, Y.; Naraoka, H.; Tomita, M.; Nishioka, T. Quantitative metabolome analysis using capillary electrophoresis mass spectrometry. *J. Proteome Res.* **2003**, *2* (5), 488−494.

(18) Gilliland, W. M.; Mellors, J. S.; Ramsey, J. M. Coupling Microchip Electrospray Ionization Devices with High Pressure Mass Spectrometry. *Anal. Chem.* **2017**, *89* (24), 13320−13325.

(19) Jeelani, G.; Sato, D.; Soga, T.; Watanabe, H.; Nozaki, T. Mass spectrometric analysis of L-cysteine metabolism: physiological role and fate of L-cysteine in the enteric protozoan parasite Entamoeba histolytica. *mBio* **2014**, *5* (6), e01995−14.

(20) Váradi, C.; Mittermayr, S.; Millán-Martín, S.; Bones, J. Quantitative twoplex glycan analysis using 12 C 6 and 13 C 6 stable isotope 2-aminobenzoic acid labelling and capillary electrophoresis mass spectrometry. *Anal. Bioanal. Chem.* **2016**, *408* (30), 8691−8700.

(21) Wang, Y.; Feng, P.; Sosic, Z.; Zang, L. Monitoring Glycosylation Profile and Protein Titer in Cell Culture Samples Using Zipchip CE−MS. *J. Anal. Bioanal. Tech.* **2017**, *8* (359), 2.
(22) Zhang, Y.; Wang, Y.; Sosic, Z.; Zang, L.; Bergelson, S.; Zhang, W. Identification of adeno-associated virus capsid proteins using ZipChip CE/MS. *Anal. Biochem.* **2018**, *555*, 22−25.
(23) Creek, D. J.; Chokkathukalam, A.; Jankevics, A.; Burgess, K. E.; Breitling, R.; Barrett, M. P. Stable isotope-assisted metabolomics for network-wide metabolic pathway elucidation. *Anal. Chem.* **2012**, *84* (20), 8442−8447.
(24) Colton, C. A.; Vitek, M. P.; Wink, D. A.; Xu, Q.; Cantillana, V.; Previti, M. L.; Van Nostrand, W. E.; Weinberg, J. B.; Dawson, H. NO synthase 2 (NOS2) deletion promotes multiple pathologies in a mouse model of Alzheimer's disease. *Proc. Natl. Acad. Sci. U. S. A.* **2006**, *103* (34), 12867−12872.
(25) Colton, C.; Wilcock, D.; Wink, D.; Davis, J.; Van Nostrand, W.; Vitek, M. The effects of NOS2 gene deletion on mice expressing mutated human AbetaPP. *J. Alzheimer's Dis.* **2008**, *15*, 571−587.
(26) Colton, C. A.; Mott, R. T.; Sharpe, H.; Xu, Q.; Van Nostrand, W. E.; Vitek, M. P. Expression profiles for macrophage alternative activation genes in AD and in mouse models of AD. *J. Neuroinflammation* **2006**, *3* (1), 27.
(27) Wilcock, D. M.; Lewis, M. R.; Van Nostrand, W. E.; Davis, J.; Previti, M. L.; Gharkholonarehe, N.; Vitek, M. P.; Colton, C. A. Progression of Amyloid Pathology to Alzheimer's Disease Pathology in an Amyloid Precursor Protein Transgenic Mouse Model by Removal of Nitric Oxide Synthase 2. *J. Neurosci.* **2008**, *28* (7), 1537−1545.
(28) Hoos, M. D.; Vitek, M. P.; Ridnour, L. A.; Wilson, J.; Jansen, M.; Everhart, A.; Wink, D. A.; Colton, C. A. The impact of human and mouse differences in NOS2 gene expression on the brain's redox and immune environment. *Mol. Neurodegener.* **2014**, *9*, 50−50.
(29) Kan, M. J.; Lee, J. E.; Wilson, J. G.; Everhart, A. L.; Brown, C. M.; Hoofnagle, A. N.; Jansen, M.; Vitek, M. P.; Gunn, M. D.; Colton, C. A. Arginine deprivation and immune suppression in a mouse model of Alzheimer's disease. *J. Neurosci.* **2015**, *35* (15), 5969−5982.
(30) Wilcock, D. M.; Lewis, M. R.; Van Nostrand, W. E.; Davis, J.; Previti, M. L.; Gharkholonarehe, N.; Vitek, M. P.; Colton, C. A. Progression of amyloid pathology to Alzheimer's disease pathology in an amyloid precursor protein transgenic mouse model by removal of nitric oxide synthase 2. *J. Neurosci.* **2008**, *28* (7), 1537−1545.
(31) Xu, J.; Begley, P.; Church, S. J.; Patassini, S.; Hollywood, K. A.; Jüllig, M.; Curtis, M. A.; Waldvogel, H. J.; Faull, R. L. M.; Unwin, R. D.; Cooper, G. J. S. Graded perturbations of metabolism in multiple regions of human brain in Alzheimer's disease: Snapshot of a pervasive metabolic disorder. *Biochim. Biophys. Acta, Mol. Basis Dis.* **2016**, *1862* (6), 1084−1092.
(32) Inoue, K.; Tsutsui, H.; Akatsu, H.; Hashizume, Y.; Matsukawa, N.; Yamamoto, T.; Toyo'oka, T. Metabolic profiling of Alzheimer's disease brains. *Sci. Rep.* **2013**, DOI: 10.1038/srep02364.
(33) Graham, S. F.; Chevallier, O. P.; Elliott, C. T.; Hölscher, C.; Johnston, J.; McGuinness, B.; Kehoe, P. G.; Passmore, A. P.; Green, B. D. Untargeted metabolomic analysis of human plasma indicates differentially affected polyamine and L-arginine metabolism in mild cognitive impairment subjects converting to Alzheimer's disease. *PLoS One* **2015**, *10* (3), e0119452.
(34) Hannibal, L. Nitric oxide homeostasis in neurodegenerative diseases. *Curr. Alzheimer Res.* **2016**, *13* (2), 135−149.
(35) Yu, J.; Kong, L.; Zhang, A.; Han, Y.; Liu, Z.; Sun, H.; Liu, L.; Wang, X. High-throughput metabolomics for discovering potential metabolite biomarkers and metabolic mechanism from the APPswe/PS1dE9 transgenic model of Alzheimer's disease. *J. Proteome Res.* **2017**, *16* (9), 3219−3228.
(36) Trushina, E.; Dutta, T.; Persson, X.-M. T.; Mielke, M. M.; Petersen, R. C. Identification of altered metabolic pathways in plasma and CSF in mild cognitive impairment and Alzheimer's disease using metabolomics. *PLoS One* **2013**, *8* (5), e63644.
(37) Vural, H.; Sirin, B.; Yilmaz, N.; Eren, I.; Delibas, N. The role of arginine−nitric oxide pathway in patients with Alzheimer disease. *Biol. Trace Elem. Res.* **2009**, *129* (1−3), 58−64.
(38) Liu, P.; Fleete, M. S.; Jing, Y.; Collie, N. D.; Curtis, M. A.; Waldvogel, H. J.; Faull, R. L.; Abraham, W. C.; Zhang, H. Altered arginine metabolism in Alzheimer's disease brains. *Neurobiol. Aging* **2014**, *35* (9), 1992−2003.
(39) Moretto, J.; Girard, C.; Demougeot, C. The role of arginase in aging: A systematic review. *Exp. Gerontol.* **2019**, *116*, 54.
(40) van Eijk, H. M. H.; Luiking, Y. C.; Deutz, N. E. P. Methods using stable isotopes to measure nitric oxide (NO) synthesis in the l-arginine/NO pathway in health and disease. *J. Chromatogr. B: Anal. Technol. Biomed. Life Sci.* **2007**, *851* (1), 172−185.
(41) Castillo, L.; Beaumier, L.; Ajami, A. M.; Young, V. R. Whole body nitric oxide synthesis in healthy men determined from [15N] arginine-to-[15N]citrulline labeling. *Proc. Natl. Acad. Sci. U. S. A.* **1996**, *93* (21), 11460−5.
(42) Siervo, M.; Stephan, B. C. M.; Feelisch, M.; Bluck, L. J. C. Measurement of in vivo nitric oxide synthesis in humans using stable isotopic methods: a systematic review. *Free Radical Biol. Med.* **2011**, *51* (4), 795−804.
(43) Weinberg, J. B.; Volkheimer, A. D.; Rubach, M. P.; Florence, S. M.; Mukemba, J. P.; Kalingonji, A. R.; Langelier, C.; Chen, Y.; Bush, M.; Yeo, T. W.; Granger, D. L.; Anstey, N. M.; Mwaikambo, E. D. Monocyte polarization in children with falciparum malaria: relationship to nitric oxide insufficiency and disease severity. *Sci. Rep.* **2016**, *6*, 29151.
(44) Barber, B. E.; William, T.; Grigg, M. J.; Piera, K. A.; Chen, Y.; Wang, H.; Weinberg, J. B.; Yeo, T. W.; Anstey, N. M. Nitric Oxide-Dependent Endothelial Dysfunction and Reduced Arginine Bioavailability in Plasmodium vivax Malaria but No Greater Increase in Intravascular Hemolysis in Severe Disease. *J. Infect. Dis.* **2016**, *214* (10), 1557−1564.
(45) Morris, S. M., Jr. Arginine Metabolism Revisited. *J. Nutr.* **2016**, *146* (12), 2579s−2586s.
(46) Xu, P. T.; Schmechel, D.; Rothrock-Christian, T.; Burkhart, D. S.; Qiu, H. L.; Popko, B.; Sullivan, P.; Maeda, N.; Saunders, A. M.; Roses, A. D.; Gilbert, J. R. Human apolipoprotein E2, E3, and E4 isoform-specific transgenic mice: human-like pattern of glial and neuronal immunoreactivity in central nervous system not observed in wild-type mice. *Neurobiol. Dis.* **1996**, *3* (3), 229−45.
(47) Bour, A.; Grootendorst, J.; Vogel, E.; Kelche, C.; Dodart, J. C.; Bales, K.; Moreau, P. H.; Sullivan, P. M.; Mathis, C. Middle-aged human apoE4 targeted-replacement mice show retention deficits on a wide range of spatial memory tasks. *Behav. Brain Res.* **2008**, *193* (2), 174−82.
(48) Wang, P. N.; Liu, H. C.; Liu, T. Y.; Chu, A.; Hong, C. J.; Lin, K. N.; Chi, C. W. Estrogen-metabolizing gene COMT polymorphism synergistic APOE epsilon4 allele increases the risk of Alzheimer disease. *Dementia Geriatr. Cognit. Disord.* **2005**, *19* (2−3), 120−5.
(49) Sullivan, P. M.; Mezdour, H.; Aratani, Y.; Knouff, C.; Najib, J.; Reddick, R. L.; Quarfordt, S. H.; Maeda, N. Targeted replacement of the mouse apolipoprotein E gene with the common human APOE3 allele enhances diet-induced hypercholesterolemia and atherosclerosis. *J. Biol. Chem.* **1997**, *272* (29), 17972−80.
(50) Mellors, J. S.; Gorbounov, V.; Ramsey, R. S.; Ramsey, J. M. Fully Integrated Glass Microfluidic Device for Performing High-Efficiency Capillary Electrophoresis and Electrospray Ionization Mass Spectrometry. *Anal. Chem.* **2008**, *80* (18), 6881−6887.
(51) Adams, K. J.; Pratt, B.; Bose, N.; Dubois, L. G.; St John-Williams, L.; Perrott, K. M.; Ky, K.; Kapahi, P.; Sharma, V.; MacCoss, M. J.; Moseley, M. A.; Colton, C. A.; MacLean, B. X.; Schilling, B.; Thompson, J. W. Skyline for Small Molecules: A Unifying Software Package for Quantitative Metabolomics. *J. Proteome Res.* **2020**, *19* (4), 1447−1458.
(52) Wu, G.; Bazer, F. W.; Cudd, T. A.; Jobgen, W. S.; Kim, S. W.; Lassala, A.; Li, P.; Matis, J. H.; Meininger, C. J.; Spencer, T. E. Pharmacokinetics and safety of arginine supplementation in animals. *J. Nutr.* **2007**, *137* (6), 1673S−1680S.

(53) Bode-Böger, S. M.; Böger, R. H.; Galland, A.; Tsikas, D.; Frölich, J. C. L-arginine-induced vasodilation in healthy humans: pharmacokinetic−pharmacodynamic relationship. *Br. J. Clin. Pharmacol.* **1998**, *46* (5), 489−497.
(54) Forte, P.; Kneale, B. J.; Milne, E.; Chowienczyk, P. J.; Johnston, A.; Benjamin, N.; Ritter, J. M. Evidence for a difference in nitric oxide biosynthesis between healthy women and men. *Hypertension* **1998**, *32* (4), 730−734.
(55) Didelija, I. C.; Mohammad, M. A.; Marini, J. C. Ablation of Arginase II Spares Arginine and Abolishes the Arginine Requirement for Growth in Male Mice. *J. Nutr.* **2017**, *147* (8), 1510−1516.

https://doi.org/10.1021/jasms.1c00055
J. Am. Soc. Mass Spectrom. XXXX, XXX, XXX−XXX